

## Research Paper

# Quantitative Atlas of Membrane Transporter Proteins: Development and Application of a Highly Sensitive Simultaneous LC/MS/MS Method Combined with Novel *In-silico* Peptide Selection Criteria

Junichi Kamiie,<sup>1,2</sup> Sumio Ohtsuki,<sup>1,2</sup> Ryo Iwase,<sup>1</sup> Ken Ohmine,<sup>1</sup> Yuki Katsukura,<sup>1,2</sup> Kazunari Yanai,<sup>1</sup> Yumi Sekine,<sup>1</sup> Yasuo Uchida,<sup>1</sup> Shingo Ito,<sup>1,2</sup> and Tetsuya Terasaki<sup>1,2,3</sup>

Received November 19, 2007; accepted January 2, 2008; published online January 25, 2008

**Purpose.** To develop an absolute quantification method for membrane proteins, and to construct a quantitative atlas of membrane transporter proteins in the blood–brain barrier, liver and kidney of mouse.

**Methods.** Mouse tissues were digested with trypsin, and mixed with stable isotope labeled-peptide as a quantitative standard. The amounts of transporter proteins were simultaneously determined by liquid chromatography–tandem mass spectrometer (LC/MS/MS).

**Results.** The target proteins were digested *in-silico*, and target peptides for analysis were chosen on the basis of the selection criteria. All of the peptides selected exhibited a detection limit of 10 fmol and linearity over at least two orders of magnitude in the calibration curve for LC/MS/MS analysis. The method was applied to obtain the expression levels of 34 transporters in liver, kidney and blood–brain barrier of mouse. The quantitative values of transporter proteins showed an excellent correlation with the values obtained with existing methods using antibodies or binding molecules.

**Conclusion.** A sensitive and simultaneous quantification method was developed for membrane proteins. By using this method, we constructed a quantitative atlas of membrane transporter proteins at the blood–brain barrier, liver and kidney in mouse. This technology is expected to have major implications for various fields of biomedical science.

**KEY WORDS:** ABC transporter; LC/MS/MS; multiple reaction monitoring (MRM); pharmacoproteomics; SLC transporter.

## INTRODUCTION

The membrane transporter protein family is one of the most important groups of proteins in clinical research and in drug discovery and development. Membrane transporters are essential for human physiological functions, and mutation of transporters is involved in various genetic diseases, including systemic carnitine deficiency (1), cystic fibrosis (2) or Dubin–Johnson syndrome (3). Transporters also play key roles in

multi-drug resistance of cancer cells by restricting the intracellular import of drugs (4). Membrane transporter proteins are expressed in tissues such as intestine, liver, and kidney, and play key roles in blood–tissue barrier function, as well as in the absorption, distribution and elimination of small molecules, including drugs, *in vivo* (5–8). In humans, 368 proteins, including 49 ATP-binding cassette transporter family members and 319 solute carrier transporter family members, have been classified as transporter proteins by the Human Genome Organization (HUGO) Gene Nomenclature Committee (URL: <http://www.genenames.org/genefamily.html>). Profiling of the transporter protein families, i.e., developing a quantitative atlas of membrane transporter proteins, in each organ or tissue of humans is fundamental for biomedical science, as well as for drug discovery and development.

The use of tandem mass spectrometry in conjunction with the genome database has allowed the large-scale identification of proteins expressed in biological and clinical materials (9–11). Several quantitative proteomics methods based on mass spectrometry have been developed for comprehensive analysis of proteins in complex mixtures (12–14) and for detection of disease biomarkers (15). However, the presently available comprehensive proteomics approaches, such as the shotgun method with multidimen-

<sup>1</sup> Division of Membrane Transport and Drug Targeting, Graduate School of Pharmaceutical Sciences, Tohoku University, Aoba, Aramaki, Aoba-ku, Sendai 980-8578, Japan.

<sup>2</sup> SORST of the Japan Science and Technology Agency, Kawaguchi, Japan.

<sup>3</sup> To whom correspondence should be addressed. (e-mail: [terasaki@mail.pharm.tohoku.ac.jp](mailto:terasaki@mail.pharm.tohoku.ac.jp))

**ABBREVIATIONS:** ABC transporters, ATP binding cassette transporters; CV, coefficient of variation; ESI, electro-spray ionization; HSA, human serum albumin; HUGO, Human Genome Organization; LC, liquid chromatography; MRM, multiple reaction monitoring; MS/MS, tandem mass spectrometry; PBS, phosphate-buffered saline; PMSF, phenylmethylsulfonyl fluoride; Q1, quadrupole 1; Q3, quadrupole 3; SLC transporters, solute carrier family of transporters.

sional LC-based mass spectrometry, are still not able to comprehensively profile human transporters. One reason for this is that functional membrane transporter proteins are often expressed at extremely low levels. In the analysis of highly complex samples by mass spectrometry, only peptides of the highest ion intensity are selected, while those of lower ion intensity pass through the system. Hence, an efficient detection method for low-expression-level proteins is required to profile functional membrane proteins.

As distinct from comprehensive proteomics, focused proteomics aims to quantify one or several target protein(s) by using a triple-quadrupole mass spectrometer with stable isotope-labeled peptides as internal references (11,16–20). The multiple reaction monitoring (MRM) mode is employed for detection (20,21). MRM analysis comprises two stages of mass selection: the first stage (Q1) selects the mass of the precursor ion and the second stage (Q3) selects the mass of a specific fragment ion derived from the precursor ion. The high selectivity resulting from the two stages of mass selection yields a very specific and sensitive measure of the target analyte in the mixture. Indeed, MRM analysis can quantify small compounds down to attomolar levels. Therefore, focused proteomics with multi-channel MRM analysis should be suitable to quantify proteins that are expressed at extremely low levels. However, no one has yet succeeded in developing a simultaneous and direct quantitation method for multiple membrane proteins. The proteolysis step for mass spectrometry-based proteomics yields a large number of peptides from each protein, and the peptides even from a single protein vary greatly in detectability. The sensitivity and selectivity of the MRM analysis consequently depend on the nature of the tryptic peptides. To date, target tryptic peptides have been determined by standard comprehensive proteomics analysis, so proteins that cannot be detected by comprehensive proteomics analysis can also not be quantified by MRM analysis. Therefore, an efficient strategy for identifying unique peptides derived from a target protein is critical for the application of MRM to quantify proteins of a specific functional protein group, such as the 368 membrane transporter proteins.

Here, we describe a high-throughput strategy that employs *in-silico* peptide selection for mass spectrometry-based quantitation of multiple membrane proteins in very complex samples, such as mammalian tissues. We applied it to focused proteomics of membrane transporter proteins, and were able for the first time to determine simultaneously the expression levels of multiple membrane transporters in mouse tissues. This method is expected to provide a quantitative atlas of membrane transporter proteins that should promote a shift in focus from pharmacogenomics to pharmacoproteomics, and this, in turn, is expected to provide greater insight into many areas of pharmaceutical and biomedical sciences.

## MATERIALS AND METHODS

### Animals

Male ddY mice (9–10 weeks of age) were purchased from Charles River (Yokohama, Japan). The experiments in this report conformed to the guidelines established by the Animal

Care Committee, Graduate School of Pharmaceutical Sciences, Tohoku University.

### Reagents

Antibody against ABCG2 was prepared as described previously (22). All peptides (Table III) were synthesized by Thermolectron Corporation (Sedanstrabe, Germany). Other chemicals were commercial products of analytical grade.

### Mouse Tissue Preparation

Mice were transcardially perfused with phosphate-buffered saline (PBS) to remove blood under deep anesthesia induced with ketamine and xylazine. Brains, livers and kidneys were then isolated. The brain capillary fraction was collected from mouse cerebrum by the glass bead column method (23). The cerebrum was dissected into 1-mm pieces and homogenized in PBS using a Potter–Elvehjem homogenizer. The homogenate was added to the same volume of 32% dextran solution, and then centrifuged (4,500×g, 10 min, 4°C). The resulting pellets were washed in PBS to give the capillary-rich fraction. This fraction was passed through an 85- $\mu$ m nylon mesh filter. The column was washed with PBS, and the brain capillary endothelial cells attached to glass beads were isolated by gentle shaking to give the brain capillary fraction. The plasma membrane fractions were prepared from liver, renal cortex and renal medulla by sucrose density gradient centrifugation. Tissues were dissected into pieces and homogenized using a Potter–Elvehjem homogenizer in buffer containing 10 mM Tris–HCl (pH 7.4), 10 mM NaCl, 1.5 mM MgCl<sub>2</sub>, 1 mM phenylmethylsulfonyl fluoride (PMSF), and a protease inhibitor cocktail (Sigma Chemical Co., St. Louis, USA). The homogenized tissues were centrifuged at 8,000×g for 10 min at 4°C and the supernatants were collected. They were centrifuged at 100,000×g for 60 min at 4°C, and the pellets were suspended in 10 mM Tris–HCl (pH 7.4), 250 mM sucrose. Each suspension was layered on top of a 38% (w/v) sucrose solution and centrifuged at 100,000×g for 40 min at 4°C. The turbid layer at the interface was recovered, diluted with 10 mM Tris–HCl (pH 7.4), 250 mM sucrose, and centrifuged at 100,000×g for 40 min at 4°C. Plasma membrane fraction was obtained from the resulting pellet, which was suspended in 10 mM Tris–HCl (pH 8.0). Protein concentrations were measured by the Lowry method using the DC protein assay reagent (Bio-Rad, Hercules, USA).

### Cytochalasin B Binding Assay

Intact brain capillary endothelial cells were incubated at 25°C for 15 min in the presence of 500 mM L-glucose or D-glucose, and varying concentrations of [<sup>3</sup>H]cytochalasin B (GE healthcare, Tokyo, Japan) (24). All samples were treated with digitonin for efficient binding of cytochalasin B to the luminal side of brain capillary endothelial cells through the plasma membrane, and incubated with 4  $\mu$ M cytochalasin E to inhibit nonspecific binding to microfilaments. The binding assays were terminated by rapid cold filtration over GF/B glass fiber filters. Specific cytochalasin B binding was calculated as the difference between the total binding in the

presence of L-glucose and D-glucose. The equilibrium constant of binding was estimated according to Scatchard.

### Immunoblotting Assay for Bcrp

Protein samples (brain capillary endothelial cells, 10 µg; plasma membranes of liver, 5 µg; plasma membranes of renal cortex and renal medulla, 1 µg per lane) were resolved by 10% SDS-polyacrylamide gel electrophoresis and electrotransferred to polyvinylidene difluoride membranes (Amersham Biosciences). These were treated with blocking buffer (4% skimmed milk in 25 mM Tris-HCl (pH 8.0), 125 mM NaCl, 0.1% Tween 20) for 1 h at room temperature and incubated with anti-ABCG2 antibodies at 4°C for 16 h. The membranes were washed three times with blocking buffer and incubated with horseradish peroxidase-conjugated antibody. Signals were visualized with an enhanced chemiluminescence kit (Immobilon™ Western Detection Reagents, Millipore, Tokyo, Japan) and its intensity was estimated with NIH image software.

### Quantitative Immunoblotting Assay for MDR1

ABCB1 partial recombinant protein (620–710 a.a.) with a GST tag (Abnova Corporation, Taiwan) was obtained as a concentration standard. The plasma membrane fraction of LLC-GA5-CoL300 cells transfected with hMDR1 cDNA was obtained by homogenization and sucrose density gradient centrifugation as the mouse tissue preparation. Dilution series of recombinant protein (300, 400, 500, 600, 700, 800, 1,000 fmol) and 2 µg of plasma membrane protein were resolved by 7.5% SDS-polyacrylamide gel electrophoresis and electrotransferred to polyvinylidene difluoride membranes (GE Healthcare, Tokyo, Japan). These were treated with blocking buffer (4% skimmed milk in 25 mM Tris-HCl [pH 8.0], 125 mM NaCl, 0.1% Tween 20) for 1 h at room temperature and incubated with monoclonal antibodies raised against a partial recombinant ABCB1 protein (Abnova Corporation, Taipei, Taiwan) at 4°C for 16 h. Signals were visualized as described above for Bcrp immunoblotting. Signal intensity was estimated with NIH Image software.

### Mass Spectrometric Analysis

Isolated brain capillary endothelial cells, liver plasma membrane, renal cortex and medulla plasma membrane of mouse were suspended in 100 mM Tris-HCl (pH 8.5), 7 M guanidium hydrochloride, 10 mM EDTA, and the proteins were S-carbamoylmethylated as described (25). The alkylated proteins were precipitated with a mixture of methanol and chloroform. The precipitates were dissolved in 6 M urea, diluted with 100 mM Tris-HCl (pH 8.0) and digested with TPCK-treated trypsin (Promega, Madison, USA) at an enzyme/substrate ratio of 1:100 at 37°C for 16 h. Efficiency of tryptic digestion was checked with SDS-PAGE followed by CBB staining.

The tryptic digests were acidified with formic acid for analysis with the HPLC system (Agilent1100 system, Agilent, Santa Clara, USA), which was connected to an ESI-triple quadrupole mass spectrometer (API5000, Applied Biosystems, Foster City, USA). HPLC was performed with C18

capillary columns (Agilent 300SB-C18 0.5 mm ID×150 mm, 5 µm particles). Linear gradients of 1–45% acetonitrile in 0.1% formic acid were applied to elute the peptides at a flow rate of 50 µl/min for 50 min. The mass spectrometer was set up to run a multi-channel reaction monitoring (MRM) experiment for peptide detection in ten dwell times per channel. The ion counts in the chromatograms were determined by using the quantitation procedures in Analyst software version 1.4.2 (Applied Biosystems).

## RESULTS

### Strategy for Quantification of Multiple Membrane Proteins by LC-MS/MS

The overall strategy for quantification of multiple membrane proteins consists of three steps (Fig. 1). In the first step, candidate peptide probes are selected among the tryptic peptides from the target proteins, using *in-silico* selection criteria (Table I), and stable isotope-labeled and unlabeled forms of the selected peptides are synthesized. In the second step, the biological sample is digested with trypsin under denaturing conditions. Known amounts of the labeled peptides are spiked into the digest as internal references, and the mixture is analyzed by LC-MS/MS in the MRM mode. Multiple products derived from single peptides are monitored in specific *m/z* channels (Fig. 1). In the final step, individual signal peaks are identified on the basis of equal retention times in each channel of multiple product ions. To obtain the amounts of target proteins, the peptides are quantified by calculating the ratios of the peak areas to those of the isotope-labeled peptides.

### Sensitivity and Quantitative Reliability of MRM Analysis of the Selected Peptides

The *in-silico* selection criteria shown in Table I were applied to 36 membrane proteins of the mouse: 15 ATP binding cassette transporters (ABC transporters), 17 members of the solute carrier family of transporters (SLC transporters), two members of the Mate family and two membrane enzymes that have been reported to function or to be expressed in brain capillary endothelial cells and/or liver and/or kidney (5,6,8). Initially, the peptides that met all the first selection criteria (Table I) were selected as candidate's peptides from the tryptic peptides of the membrane proteins. Secondly, peptides specific for each target membrane protein were selected by NCBI BLAST search against the mouse database. As a result, 2–32 specific candidate peptides were extracted from 21 to 163 possible tryptic peptides (Table II). Finally, a single peptide fitting as many of the second selection criteria as possible was selected as the probe peptide for quantification. The selected probe peptides were synthesized as sets of stable isotope-labeled and unlabeled forms. We synthesized two sets of probe peptides for each of mouse Mdr1a and Bcrp, in order to examine the dependence of quantitative values on peptide sequence and location within the protein. Table III shows the amino acid sequences and *m/z* values of the precursor ion and three product ions for each of the 38 probe peptide sets for the 36 membrane proteins, including unlabeled and labeled forms.

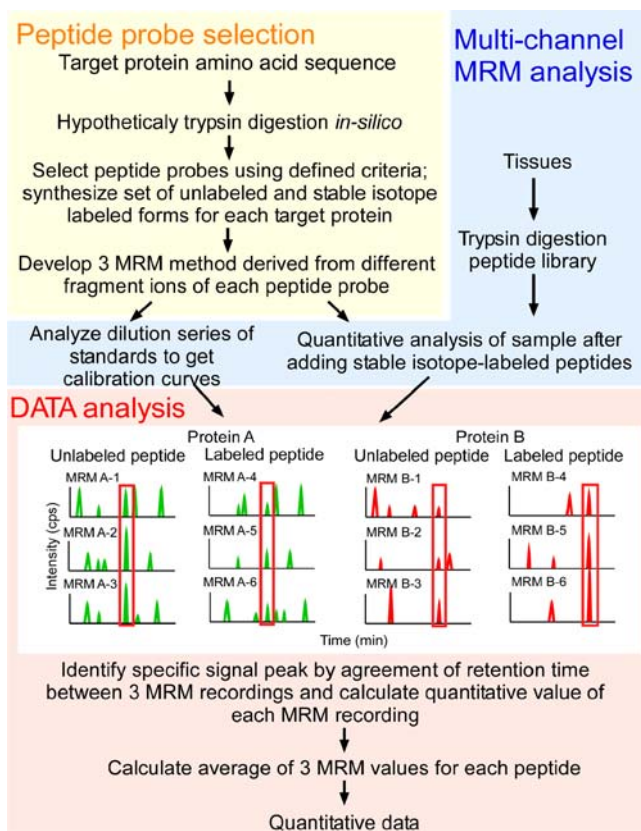


**Fig. 1.** Schematic representation of the protein quantification strategy. Quantification strategy is composed by three section including *in-silico* peptide selection (yellow zone), Multi-channel MRM analysis (blue zone) and DATA analysis (red zone). Target proteins are hypothetically digested with trypsin and detectable peptides in LC-MS/MS are selected by means of an informatics approach. Selected peptides are synthesized as sets of unlabeled and stable isotope-labeled forms. Analysis of three product ions of each peptide is optimized with LC-MS/MS in the MRM mode. A biological sample is digested with trypsin under denaturing conditions. The digest is mixed with a fixed amount of stable isotope-labeled peptides as internal standards and analyzed by LC-MS/MS in the MRM mode. Specific signal peaks are identified by the agreement of retention time among the channels. The quantity of target proteins is calculated from the peak area ratio (endogenous peptide/stable isotope-labeled peptide).

To evaluate the sensitivity and accuracy in the MRM analysis of the selected peptides, the means and the coefficients of variation (CV) of peak areas of the selected peptides were compared with those of all tryptic peptides of human serum albumin (HSA, Fig. 2). All 38 peptides selected with the *in-silico* selection criteria were detected at the level of 10 fmol with peak areas of greater than  $1.8 \times 10^3$  counts (closed circles). Moreover 28 of the peptides (74%) had peak areas of greater than  $5.0 \times 10^3$  cps and CVs of less than 40%. In contrast, 53 of the 85 peptides (62%) from HSA were detected at 10 fmol by MRM analysis (open circles), and only ten of them (12%) had peak areas of greater than  $5 \times 10^3$  counts. The ratios of peak areas of unlabeled to stable isotope-labeled forms for 13 different peptides were linearly correlated to the mixing ratio in the range from 10:200 to 1,000:200 (unlabeled form *versus* labeled form), and the regression line of peak area ratio against mixing ratio was described by the equation  $y=1.00x-0.02$  ( $R^2=1.00$ ; Fig. 3).

These results indicate that MRM analysis has at least a 100-fold dynamic range.

### Signal Peak Identification By Multi-channel MRM Analysis

Since noise peaks are detected in the analysis of biological samples, the signal peak must be identified among a number of noise peaks. To identify the signal peak, six MRM channels (three channels each for the unlabeled peptide and the labeled peptide) were established for one set of probe peptides, and the signal peak was identified by virtue of the agreement of the retention times in the six MRM channels. Figure 4A and B show MS/MS spectra of the unlabeled probe peptide of mouse Mdr1a (NTTGALTR) and the corresponding labeled peptide (NTTGAL( $^{13}\text{C}_6$ ,  $^{15}\text{N}$ )TTR), respectively, obtained by direct injection at the 1  $\mu\text{M}$  level in the product ion scan (MS2) mode. Six ions of the y series (y3–y8) were detected at over  $5.0 \times 10^4$  cps in both the unlabeled and labeled forms, although only b2 was detected in the b series. The ions which gave high peak intensities in the MS/MS spectrum (y5, y6 and y7) were selected for the multi-channel MRM, and the  $m/z$  values of the product ion-1, product ion-2 and product ion-3 of Mdr1a shown in Table III correspond to those of y5, y6 and y7, respectively. Each MRM channel, with the  $m/z$  values of the doubly charged precursor ions and selected y-series ions as Q1 and Q3 values, was optimized for collision gas, collision energy and declustering potential to produce peak intensities of over  $0.5 \times 10^4$  cps at the 1  $\mu\text{M}$  level for the target probe peptide. Since the peptide sequence of the probe peptide selected is conserved in human MDR1, when the plasma membrane fraction of MDR1-expressing cells was analyzed using the established multi-channel MRM simultaneously, a peak at 24.9 min were detected in all six MRM channels, and identified as being due to NTTGALTTR (Fig. 4C).

### Simultaneous Quantitative Analysis of 36 Membrane Proteins in Mouse Tissues

By using the established multi-channel MRM (Table III), a simultaneous quantitative analysis of 36 mouse membrane proteins was conducted with 216 MRM channels in brain

**Table I.** Peptide Selection Criteria

Criteria for first selection (requirements)	
<b>For detection using mass spectrometry</b>	
Length between 6 and 16 amino acids	
No posttranslational modifications	
No single nucleotide polymorphism	
<b>For complete digestion with trypsin</b>	
No transmembrane region	
No continuous sequence of arginine or lysine in digestion region	
<b>For stability of peptide</b>	
No methionine or cysteine residues	
<b>For stable isotope labeling</b>	
Containing one of leucine, isoleucine, valine, alanine or proline residue	
Criteria for second selection (additional conditions)	
Length between 8 and 10 amino acids	
No histidine residue	

**Table II.** The Number of Target Peptide Candidates Selected By *In-silico* Selection Criteria

Uni-Prot Accession No.	Synonyms	Number of Tryptic Peptides	Number of Candidates from First Selection	Number of Specific Candidates
P21447	Mdr1a	139	30	17
P06795	Mdr1b	132	32	17
P21440	Mdr2	141	37	27
Q9QY30	Bsep	138	28	28
O35379	Mrp1	146	32	26
Q8VI47	Mrp2	163	27	24
Q56PH0	Mrp3	123	32	28
Q3TZN9	Mrp4	139	34	32
Q9R1X5	Mrp5	160	30	25
Q9R1S7	Mrp6	126	19	17
Q8R4P9	Mrp7	110	31	27
Q80WJ6	Mrp9	138	20	18
Q7TMS5	Bcrp	60	15	12
Q99PE8	Abcg5	59	15	14
Q7TSR7	Abcg8	55	10	10
Q9WTW5	Oct3	45	6	6
P10852	4F2hc	53	16	15
P51912	Asct2	46	9	9
Q3UNC8	Ata2	38	3	3
Q8R1S9	Nat	34	4	4
P31651	Gat2	39	2	2
P17809	Glut1	36	7	7
P53986	Mct1	32	6	6
Q9Z127	Lat1	29	4	4
O55192	Net	36	6	5
O08705	Ntcp	21	3	3
Q61185	Oat1	41	9	7
O88909	Oat3	38	7	6
Q9QXZ6	Oatp1	65	10	8
Q9EP96	Oatp2	54	4	2
Q9ERB5	Oatpf	65	8	8
O35316	Taut	41	8	7
Q3V050	Mate1	37	10	8
Q5SS45	Mate2 homolog	34	3	3
Q64436	Atp4a	96	18	14
Q60928	Ggt1	53	17	15

Target protein sequences were hypothetically digested with trypsin. Target peptide candidates for quantitative analysis were selected on the basis of *in-silico* selection criteria (Table I). Specific peptide sequences were extracted with NCBI-BLAST search from selected candidates.

capillary endothelial cells, and in the plasma membrane fractions of liver, renal cortex and renal medulla.

Typical results are shown in Fig. 5 and Table IV, which represent the MRM chromatograms and quantification values, respectively, of the Bcrp probe peptide (SLLDVLAAR). Figure 5 shows MRM chromatograms for the six MRM channels of this peptide (SLLDVLAAR; A–C, unlabeled form; D–F, isotope-labeled form) in plasma membrane fraction of mouse liver. Although many peaks were observed in each MRM chromatogram, only one peak gave the same retention time (45.7 min) in all the MRM chromatograms, and this was identified as a specific signal peak derived from the probe peptide.

The amount of each transporter protein was determined as the average of 18 quantification values; that is, from three different MRM channels of six samples. Table IV shows the quantitative values determined from individual MRM channels for Bcrp in liver samples with the probe peptide SLLDVLAAR. The mean values based on MRM channels with Q3 *m/z* values of 757.5, 644.4, and 529.3 were 8.12, 9.47,

and 8.94 fmol/ $\mu$ g protein, respectively, and there is no significant difference among these mean values ( $p > 0.05$ ). The average protein amount was determined as 8.84 fmol/ $\mu$ g protein and the CV was 10.6%.

The amounts of Mdr1a and Bcrp were measured by using two different probe peptides. The probe peptides of Mdr1a were NTTGALTTR (amino acid residue from 805 to 813) and ATVSASHIIR (amino acid residue from 997 to 1,006), which are located at the fourth cytoplasmic loop and the C-terminal cytoplasmic domain, respectively. The probe peptides of Bcrp were SLLDVLAAR (amino acid residue from 86 to 95) and ENLQFSAALR (amino acid residue from 137 to 146), which are located at the N-terminal cytoplasmic domain. The amounts of Bcrp protein determined using the two peptide probes (SLLDVLAAR and ENLQFSAALR) were not significantly different in any of the tissues examined (Table V). The amount of Mdr1a protein was determined in brain capillary endothelial cells, and again the amounts determined with the two probes (NTTGALTTR and ATVSASHIIR) were not significantly different (Table V).

**Table III.** Peptide Probe Sequences and Selected Ions for Quantification of Each Protein with LC-MS/MS in the MRM Mode

Uni-Prot Accession No.	Synonym (Gene Name)	Probe Sequence	Peptide Mass	MRM Channel ( <i>m/z</i> )			
				Q1	Q3-1	Q3-2	Q3-3
P21447	Mdr1a (Abcb1a)	NTTGALTTR	933.5	467.8	561.3	618.4	719.4
		NTTGAL*TTR	940.5	471.3	568.3	625.4	726.4
		ATVSASHIIR	1,053.6	527.8	696.4	783.4	882.5
		ATVSASHI*IR	1,060.6	531.3	703.4	790.4	889.5
P06795	Mdr1b (Abcb1b)	EAVDEDVPLVDFWR	1,660.8	831.4	807.5	904.5	1,003.6
		EAVDEDVPLVDF*WR	1,670.8	836.4	817.5	914.5	1,013.6
P21440	Mdr2 (Abcb4)	IATEAIENIR	1,128.6	565.5	644.4	715.6	844.5
		IATEA*IENIR	1,132.6	567.4	648.4	719.6	849.5
Q9QY30	Bsep (Abcb11)	STALQLIQR	1,029.0	515.5	657.5	770.5	841.5
		STALQL*IQR	1,036.0	519.0	664.6	777.5	848.5
O35379	Mrp1 (Abcc1)	TPSGNLVNR	956.5	479.3	615.4	672.4	759.4
		TPSGNL*VNR	963.5	482.8	622.4	679.4	766.4
Q8VI47	Mrp2 (Abcc2)	LTIIQDPILFSGNLR	1,796.0	899.0	693.4	806.5	1,016.6
		LTIIQDPILFSGNL*R	1,803.0	902.5	700.4	813.5	1,023.6
Q56PH0	Mrp3 (Abcc3)	ILSALAEKG	900.5	451.3	588.3	675.4	788.5
		ILSAL*AEGK	907.5	454.8	595.3	682.4	795.5
Q3TZN9	Mrp4 (Abcc4)	APVLFDFR	963.5	482.8	584.3	697.4	796.4
		APVL*FFDR	970.5	486.3	584.3	704.4	803.4
Q9R1X5	Mrp5 (Abcc5)	SLSEASVAVDR	1,132.6	567.3	646.4	717.4	933.5
		SL*SEASVAVDR	1,139.6	570.8	646.4	717.4	933.5
Q9R1S7	Mrp6 (Abcc6)	SLLWDVAR	958.5	480.3	460.3	646.3	759.4
		SLL*WDVAR	965.5	483.8	460.3	646.3	766.4
Q8R4P9	Mrp7 (Abcc10)	SEGAVALHVYR	1,200.6	601.3	857.5	928.5	985.6
		SEGAVAL*HVYR	1,207.6	604.8	864.5	935.5	992.6
Q80WJ6	Mrp9 (Abcc12)	F TSAELLR	935.5	468.8	601.4	688.4	789.4
		F TSAELL*R	942.5	472.3	608.4	695.4	796.4
Q7TMS5	Bcrp (Abcg2)	ENLQFSAALR	1,147.6	574.8	664.4	792.4	905.5
		ENLQFSAAL*R	1,154.6	578.3	671.4	799.4	912.5
		SLLLDVLAAR	1,043.6	522.8	529.3	644.4	757.5
		SLLLDVL*AAR	1,050.6	526.3	536.3	651.4	764.5
Q99PE8	Abcg5 (Abcg5)	TTLDDAISGR	1,045.6	523.8	618.3	731.4	844.5
		TTL*DAISGR	1,052.6	527.3	618.3	738.4	851.5
Q7TSR7	Abcg8 (Abcg8)	ASLLDVITGR	1,043.6	522.8	545.3	660.4	773.5
		ASLL*DVITGR	1,050.6	526.3	545.3	660.4	780.5
Q9WTW5	Oct3 (Slc22a3)	FLOGVFGK	895.1	448.3	507.3	635.4	748.4
		FLOGVF*GK	905.1	453.3	517.3	645.4	361.2
P10852	4F2hc (Slc3a2)	IGDLQAFVGR	1,074.6	538.3	478.3	549.3	677.4
		IGDLQAFV*GR	1,080.6	541.3	484.3	555.3	683.4
Q9ESU7	Asct2 (Slc1a5)	EVLDSFLDLVR	1,304.7	653.4	615.4	964.5	1,077.6
		EVLDSFLDL*VVR	1,311.7	656.9	622.4	971.5	1,084.6
Q8CD21	Ata2 (Slc38a2)	AYGLAGK	678.4	340.2	275.2	445.3	608.3
		AYGLA*GK	682.4	342.2	279.2	449.3	612.3
Q8R1S9	Nat (Slc38a4)	TSVITLLFPR	1,145.7	573.9	532.3	746.5	859.5
		TSVITLLFP*R	1,151.7	576.9	538.3	752.5	865.5
P31651	Gat2 (Slc6a12)	QELIAWEK	1,015.5	508.8	533.3	646.4	759.4
		QELIA*WEK	1,019.5	510.8	537.3	650.4	763.4
P17809	Glut1 (Slc2a1)	TFDEIASGFR	1,141.5	571.8	650.4	779.4	894.4
		TFDEI A*SGFR	1,145.5	573.8	654.4	783.4	898.4
P53986	Mct1 (Slc16a1)	SDANTDLIGGSPK	1,273.6	637.8	558.3	786.4	887.5
		SDANTDL*IGGSPK	1,280.6	641.3	558.3	793.4	894.5
Q9Z127	Lat1 (Slc7a5)	VQDAFAAAK	919.5	460.8	578.3	693.4	821.4
		VQDAFAA*AK	923.5	462.8	582.3	697.4	825.4
O55192	Net (Slc6a2)	TADLLVVK	857.5	429.8	345.2	686.4	757.5
		TADLL*VVK	864.5	433.3	345.2	693.4	764.5
O08705	Ntcp (Slc10a1)	GIYDGDLLK	879.4	440.7	432.2	547.3	710.3
		GIYDGDLL*K	886.4	444.2	439.2	554.3	717.3
Q8VC69	Oat1 (Slc22a6)	TSLAVLGK	787.5	394.8	416.3	487.3	600.4
		TSLAVL*GK	794.5	398.3	423.3	494.3	607.4
O88909	Oat3 (Slc22a8)	YGLSDLFR	969.5	485.8	637.3	750.4	807.4
		YGLSDL*FR	976.5	489.3	644.3	757.4	814.4
Q9QXZ6	Oatp1 (Slco1a1)	GVQHPLYGEK	1,126.6	564.3	496.2	706.3	843.4
		GVQHPL*YGEK	1,133.6	567.8	496.2	713.4	850.4

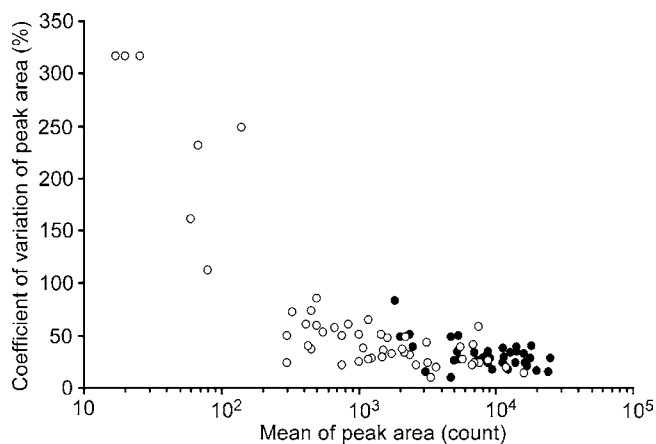
Table III. (continued)

Uni-Prot Accession No.	Synonym (Gene Name)	Probe Sequence	Peptide Mass	MRM Channel ( <i>m/z</i> )			
				Q1	Q3-1	Q3-2	Q3-3
Q9EP96	Oatp2 (Slco1a4)	EVATHGVR	867.5	434.7	468.3	569.3	640.4
		EVATHGV*R	873.5	437.7	474.3	575.3	646.4
Q9ERB5	Oatpf (SLCO1C1)	STVTQIER	932.5	467.3	417.2	545.3	646.4
		STV*TQIER	938.5	470.3	417.2	545.3	646.4
O35316	Taut (Slc6a6)	EGATPFHSR	1,000.5	501.2	399.2	546.3	643.3
		EGATPF*HSR	1,010.5	506.2	399.2	556.3	653.3
Q3V050	Mate1 (14933429E10Rik)	HVGVILQR	920.6	461.3	529.3	685.4	784.5
		HVGVIL*QR	927.6	464.8	536.3	692.4	791.5
Q5SS45	Mate 2 homolog (1300013J15Rik)	VGNALGAGNADQAR	1,312.6	657.3	731.3	802.4	859.4
		VGNALGAGNADQA*R	1,316.6	659.3	735.3	806.4	863.4
Q64436	Na <sup>+</sup> /K <sup>+</sup> ATPase (Atp4a)	VDNSSLTGESEPTQR	1,618.7	810.4	717.4	903.4	1,004.5
		VDNSSLTGESEP*QTR	1,624.7	813.4	723.4	909.4	1,010.5
Q60928	Ggt (Ggt1)	LFQPSIQLAR	1,171.7	586.8	487.3	687.4	912.5
		LFQPSIQL*AR	1,178.7	590.3	494.3	694.8	919.5

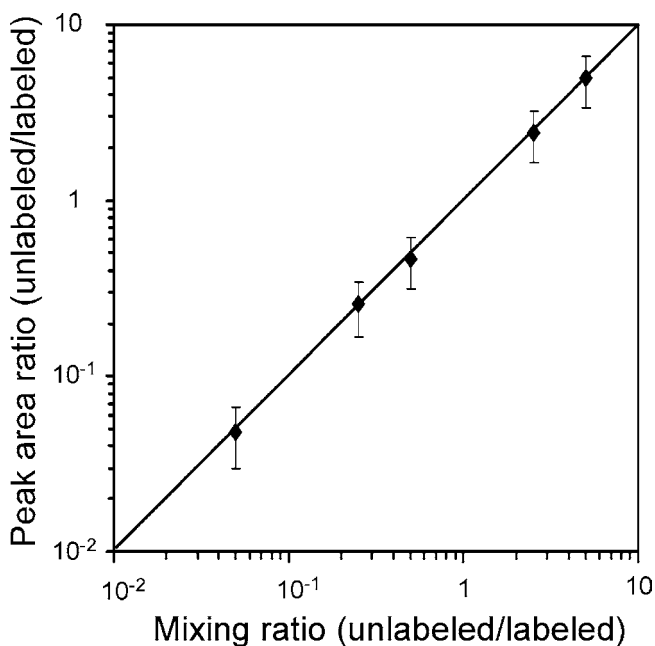
The selected peptides were synthesized and their purity was checked with HPLC-UV. The conditions of MRM were optimized for high signal intensity following direct injection of peptide solution into the mass spectrometer through a turbo ion spray source. Theoretical *m/z* values of doubly charged ions of intact peptides were assumed as precursor ions. Three singly charged fragment ions derived from the y or b series were obtained by MS/MS. Bold letters with asterisks indicate amino acid residues labeled with stable isotope (<sup>13</sup>C and <sup>15</sup>N).

Table V summarizes the quantitative mean values and CVs of all 36 membrane proteins. In brain capillary endothelial cells, the amounts of Mdr1a, Mrp4, Bcrp, 4F2hc, Asct2, Glut1, Mct1, Lat1, Oat3, Oatp2, Oatpf, Taut, Atp4a and Ggt1 were in the range from 1.59 to 90.0 fmol/μg protein, with CVs under 19.7%. In the plasma membrane fraction of liver, the amounts of Bsep, Mrp2, Mrp3, Mrp6, Bcrp, Abcg5, Abcg8, 4F2hc, Nat, Gat2, Glut1, Mct1, Ntcp, Oatp1, Oatp2 and Atp4a were in the range from 1.65 to 42.9 fmol/μg protein, with CVs under 13.6%. In plasma membrane fraction of the renal cortex, the amounts of Mrp2, Mrp4, Bcrp, 4F2hc, Asct2, Mct1, Oat1, Oat3, Oatp1, Taut, Mate1, Atp4a and Ggt1 were in the range from 0.22 to 254 fmol/μg protein, with CVs of under 18.0%, and in plasma membrane of the renal medulla,

the amounts of Mrp4, Bcrp, 4F2hc, Asct2, Glut1, Mct1, Oat1, Oat3, Oatp1, Taut, Mate1, Atp4a and Ggt1 were in the range from 0.72 to 559 fmol/μg protein, with CVs under 13.8% (Table V).



**Fig. 2.** Comparison of the means and coefficients of variation of the peak areas between 38 peptides selected based on *in-silico* criteria (closed circles) and all tryptic peptides of HSA (open circles). Thirty-eight selected peptides (10 fmol) and HSA tryptic digest were measured by MRM analysis with single MRM channel which were composed by *m/z* of doubly charged precursor ion and a single charged y series ion less than 1,000 *m/z* ( $n=8$ ).



**Fig. 3.** Correlation between peak area ratio and mixing ratio of 13 sets of unlabeled and labeled peptides. A mixture of 13 stable isotope-labeled peptides of Mdr1a probe1, Mdr1a probe2, Mrp1, Mrp2, Mrp3, Mrp4, Mrp5, Mrp6, Mrp7, Mrp9, Bcrp probe1, Bcrp probe2, Glut1 (200 fmol) was spiked with a mixture of 13 unlabeled peptides (10, 50, 100, 500, or 1,000 fmol). Each mixture was injected into the LC-MS/MS and measured, using a separate MRM channel for each peptide. Peak area ratios were calculated from the peak areas of unlabeled and stable isotope-labeled peptides (unlabeled/labeled). Each point represents the mean  $\pm$  SEM ( $n=13$ ).

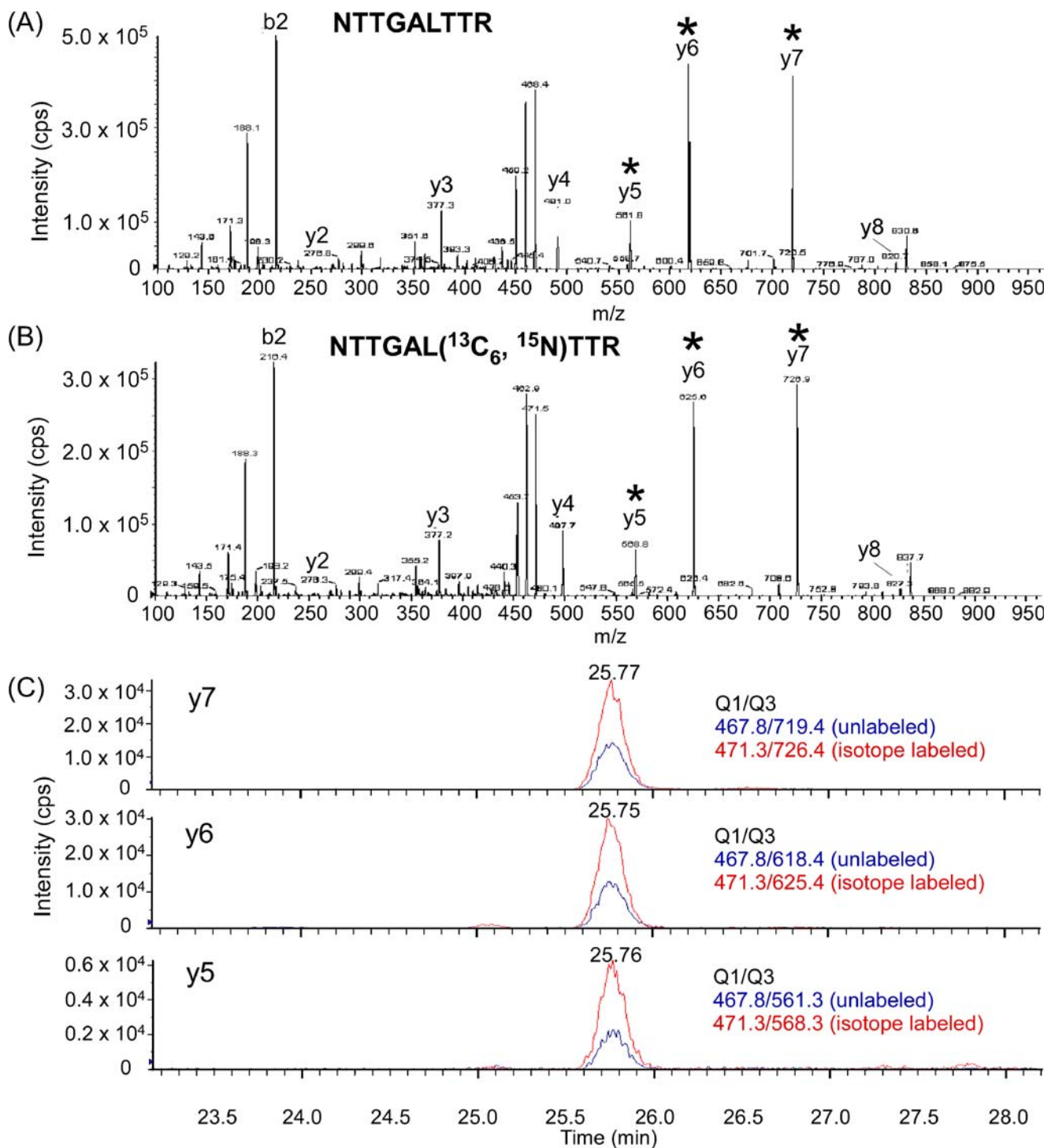


**Fig. 4.** Identification of Mdr1a/MDR1 probe peptide by multi-channel MRM analysis. **A, B** MS/MS spectrum of unlabeled (**A**) and stable isotope-labeled probe peptide (**B**) for Mdr1a/MDR1. Each peptide (1  $\mu\text{M}$ ) was infused directly into the LC-MS/MS and product ion scan (MS2) analyses were performed. The  $m/z$  of the doubly charged precursor ions and each y series ion were selected as Q1 and Q3 in the MRM channels for  $y^5$ ,  $y^6$  or  $y^7$ . Asterisks indicates product ions selected for MRM channels. **C** MRM chromatograms of Mdr1a/MDR1 probe peptide in human MDR1-expressing cells. Plasma membrane protein (1  $\mu\text{g}$ ) of human MDR1-expressing cells spiked with 200 fmol of stable isotope-labeled peptide was injected into the LC-MS/MS and simultaneous measurements were made with multi-channel MRM. Blue and red lines represent MRM chromatogram of unlabeled peptide and labeled peptide, respectively.

#### Validation of Multi-channel MRM Analysis

The accuracy of the quantitative values obtained by multi-channel MRM analysis was validated by comparison

with the values obtained with previously established methods; cytochalasin B binding assay for Glut1 and quantitative immunoblotting assay for MDR1 and Bcrp. As shown in Fig. 6A, the quantitative values for Glut1 determined by



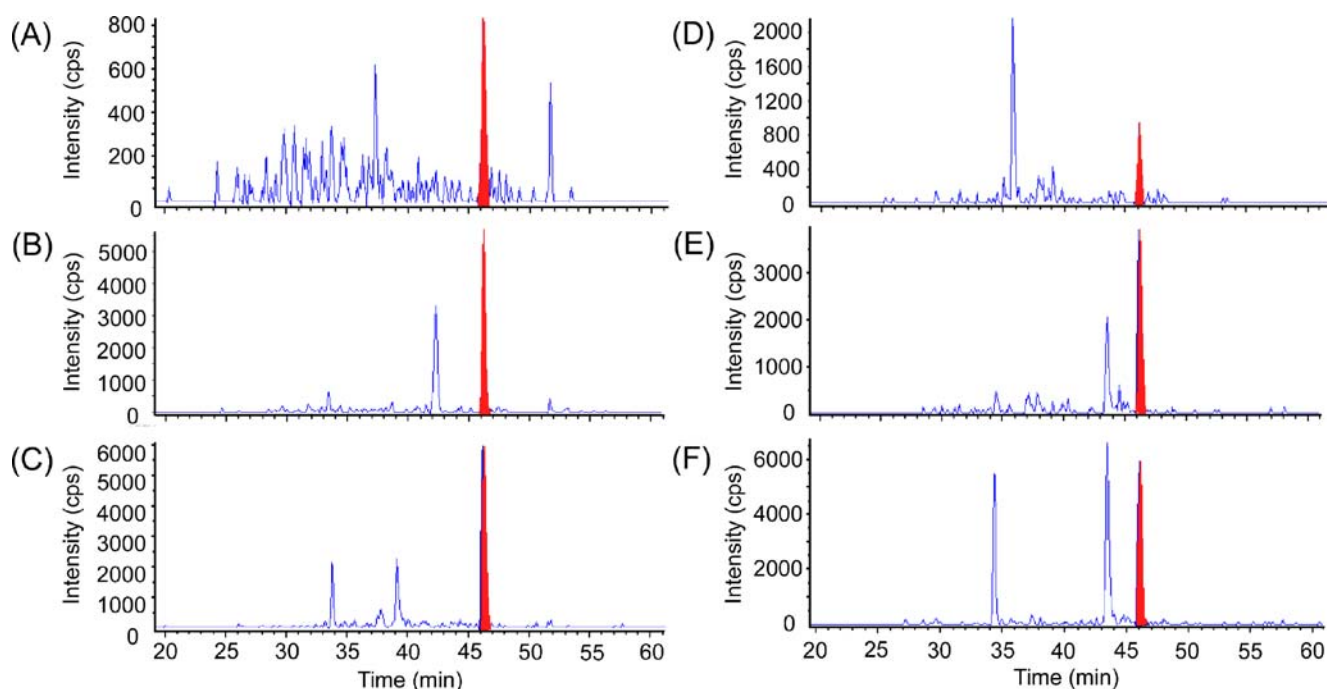


**Fig. 5.** Identification of Bcrp signal peak in plasma membrane fraction of mouse liver by means of multi-channel MRM analysis. Tryptic digests of plasma membrane fraction of mouse liver (23  $\mu$ g) spiked with stable isotope-labeled peptide mixture (200 fmol) were analyzed by multi-channel MRM analysis. **A–C** MRM chromatograms of three MRM channels for non-labeled peptide (SSLLDVLAAR) of Bcrp. **D–F** MRM chromatograms of three MRM channels for labeled peptide (SSLLDVL( $^{13}\text{C}_6$ ,  $^{15}\text{N}$ )AAR). Red-filled peaks are the peaks identified as specific signals at 45.7 min. The  $m/z$  values (Q1/Q3) of the MRMs are **A:** 522.8/757.5, **B:** 522.8/644.4, **C:** 522.8/529.3, **D:** 526.3/764.5, **E:** 526.3/651.4, **F:** 526.3/536.3.

multi-channel MRM analysis agreed with those obtained by the cytochalasin B binding assay over the range of 10–500 fmol in various amounts of mouse brain capillary endothelial cells. The amount of human MDR1 in the MDR1-expressing cultured cells was determined by quantitative immunoblotting assay with the recombinant protein, which is a partial peptide of MDR1 includes the antibody epitope. The values obtained for MDR1 were  $128 \pm 12.5$  fmol/ $\mu$ g protein by immunoblotting, and  $101 \pm 3.23$  fmol/ $\mu$ g protein by multi-channel MRM analysis, and no significant difference was observed ( $p > 0.05$ ; Fig. 6B). The signal ratios of Bcrp obtained for each tissue by immunoblotting were compared those determined by multi-channel MRM analysis with two peptide probes (Fig. 6C). When calculated as relative ratios to the levels in brain capillary endothelial cells, the Bcrp levels in liver, renal cortexes and renal medullas obtained by immunoblotting were  $2.28 \pm 0.23$ ,

$12.5 \pm 1.72$ ,  $5.87 \pm 0.88$ ; those by multi-channel MRM analysis with Bcrp peptide1 were  $2.14 \pm 0.22$ ,  $14.1 \pm 1.48$ ,  $6.79 \pm 0.95$ , and those with Bcrp peptide2 were  $1.85 \pm 0.07$ ,  $11.1 \pm 0.38$ ,  $4.92 \pm 0.14$ , respectively; no significant difference was observed ( $p > 0.05$ ).

To evaluate reproducibility, two separate multi-channel MRM analyses of the 36 membrane proteins were performed for two digests from single samples of brain capillary endothelial cells, and liver and renal cortex membranes, and the mean quantitative values obtained from each analysis were compared (Fig. 7). The ratio of quantitative values between two digests of brain capillary endothelial cells, liver plasma membrane and renal cortex plasmamembrane sample were  $0.73 \pm 0.05$ ,  $0.97 \pm 0.03$  and  $1.01 \pm 0.03$ , respectively. Each quantitative value was plotted against two digests and demonstrating excellent reproducibility of multi-channel MRM analysis (Fig. 7).

**Table IV.** Quantitative Values of Bcrp in Plasma Membrane Fraction of Liver Determined From Individual MRM Channels

$m/z$ of Q3	Quantitative Value (fmol/ $\mu$ g protein)						Average in Channel	SEM	CV (%)
	Exp.1	Exp.2	Exp.3	Exp.4	Exp.5	Exp.6			
757.5	9.39	8.61	7.83	7.30	8.61	6.96	8.12	0.41	11.3
644.4	8.43	10.5	9.35	9.57	9.52	9.43	9.47	0.30	7.01
529.3	9.30	9.87	9.57	7.91	8.22	8.78	8.94	0.35	8.65
Average in experiment	9.04	9.67	8.91	8.26	8.78	8.39	8.84	0.23	10.6

Average of quantitative values in each channel was calculated from six different analyses ( $n=6$ ). Average of quantitative values in each experiment was calculated from three different MRM channels ( $n=3$ ). Italicized letters mean the amount of Bcrp protein which were calculated from 18 quantitative values, from three different MRM channels of six samples ( $n=18$ ; three MRM channels for six samples).

**Table V.** Quantitative Values of 36 Membrane Proteins in Mouse Tissues

Synonyms	Brain Capillaries		Plasma Membrane of Liver		Plasma Membrane of Renal Cortex		Plasma Membrane of Renal Medulla	
	Mean±SEM (fmol/μg protein)	CV (%)	Mean±SEM (fmol/μg protein)	CV (%)	Mean±SEM (fmol/μg protein)	CV (%)	Mean±SEM (fmol/μg protein)	CV (%)
Mdr1a (peptide1)	15.5±0.84	8.00	N.D.	–	N.D.	–	N.D.	–
Mdr1a (peptide2)	12.7±0.53	5.94	N.D.	–	N.D.	–	N.D.	–
Mdr1b	N.D.	–	N.D.	–	N.D.	–	N.D.	–
Mdr2	N.D.	–	N.D.	–	N.D.	–	N.D.	–
Bsep	N.D.	–	6.65±0.19	7.83	N.D.	–	N.D.	–
Mrp1	N.D.	–	N.D.	–	N.D.	–	N.D.	–
Mrp2	N.D.	–	7.05±0.62	12.7	4.94±0.48	13.5	N.D.	–
Mrp3	N.D.	–	3.64±0.54	6.35	N.D.	–	N.D.	–
Mrp4	1.59±0.07	13.8	N.D.	–	0.22±0.04	16.0	0.72±0.05	10.7
Mrp5	N.D.	–	N.D.	–	N.D.	–	N.D.	–
Mrp6	N.D.	–	5.11±0.18	7.41	N.D.	–	N.D.	–
Mrp7	N.D.	–	N.D.	–	N.D.	–	N.D.	–
Mrp9	N.D.	–	N.D.	–	N.D.	–	N.D.	–
Bcrp (peptide1)	4.02±0.29	17.5	8.18±0.40	11.9	56.4±1.82	7.56	25.9±1.35	13.8
Bcrp (peptide2)	4.80±0.15	4.35	8.84±0.22	10.6	53.4±1.62	8.01	23.8±0.95	5.49
Abcg5	N.D.	–	2.82±0.19	9.09	N.D.	–	N.D.	–
Abcg8	N.D.	–	3.54±0.12	4.52	N.D.	–	N.D.	–
Oct3	N.D.	–	N.D.	–	N.D.	–	N.D.	–
4F2hc	16.4±0.34	6.67	2.06±0.08	8.29	20.9±0.70	15.7	9.61±0.31	6.41
Asct2	1.58±0.13	3.94	N.D.	–	2.21±0.10	10.1	3.09±0.12	9.01
Ata2	N.D.	–	N.D.	–	N.D.	–	N.D.	–
Nat	N.D.	–	10.3±0.23	3.67	N.D.	–	N.D.	–
Gat2	N.D.	–	2.79±0.14	7.53	N.D.	–	N.D.	–
Glut1	90.0±2.87	5.00	1.87±0.17	13.6	N.D.	–	40.4±1.83	5.21
Mct1	23.7±0.87	6.74	18.8±0.66	6.97	9.51±0.38	10.9	4.37±0.18	7.65
Lat1	2.19±0.09	9.71	N.D.	–	N.D.	–	N.D.	–
Net	N.D.	–	N.D.	–	N.D.	–	N.D.	–
Ntcp	N.D.	–	17.1±1.15	9.75	N.D.	–	N.D.	–
Oat1	N.D.	–	N.D.	–	12.7±0.60	4.33	3.00±0.16	6.91
Oat3	1.97±0.07	5.37	N.D.	–	4.66±0.14	4.98	0.94±0.07	7.14
Oatp1	N.D.	–	42.9±2.57	5.06	12.1±0.79	18.0	2.86±0.17	7.11
Oatp2	2.11±0.12	13.2	1.65±0.14	8.65	N.D.	–	N.D.	–
Oatpf	2.41±0.16	10.4	N.D.	–	N.D.	–	N.D.	–
Taut	3.81±0.60	16.7	N.D.	–	3.20±0.27	6.96	4.95±0.25	11.1
Mate1	N.D.	–	N.D.	–	6.35±0.34	11.8	1.37±0.20	9.30
Mate2 homolog	N.D.	–	N.D.	–	N.D.	–	N.D.	–
Atpa4	39.4±1.01	5.55	33.5±1.06	9.12	254±7.55	4.61	559±26.1	9.96
Ggt1	4.37±0.25	19.7	N.D.	–	180±8.16	13.4	81.1±5.25	12.8

Whole tissue proteins of brain capillaries (22 μg), plasma membrane fraction of liver (23 μg), plasma membrane fraction of renal cortex (25 μg) and medulla (40 μg) of mouse were digested with trypsin. Tryptic digests of each tissue supplemented with 200 fmol of stable isotope-labeled peptide mixture were injected into the LC-MS/MS. Multi-channel MRM analysis (108 MRM channels) was performed under optimized conditions. The quantitative value was calculated from the peak area ratio of analyte and stable isotope-labeled peptide in each MRM channel. The amount of each protein was determined as average of 18 quantitative values, from three different MRM channels of six samples with signal peaks over 5,000 counts. Each value represents the mean±S.E.M. ( $n=18$ ; three MRM channels for six samples). When more than one among three MRM channels gave no signal peak, the mean quantitative value was not determined (*N.D.*).

## DISCUSSION

We have developed a novel method for quantitative focused proteomics using *in-silico* peptide selection criteria and multi-channel MRM analysis, and applied it to construct a quantitative atlas of membrane transporter proteins in brain capillary endothelial cells, liver plasma membrane, renal cortex and renal medulla plasma membrane of the mouse.

Comprehensive analysis with the sequence-tag method can identify hundreds to thousands of proteins in biological materials in single measurement (26–28), but there limitations

in its ability to detect and identify proteins expressed at very low levels, though such proteins play important roles in many biological processes. MRM-based quantitative proteomics with stable isotope-labeled peptides as internal references is suitable for analyzing such proteins with high sensitivity. This approach has been applied to C-reactive proteins (29), growth hormone (30) and prostate-specific antigen (31). Rhodopsin, an integral membrane protein has also been measured by means of this approach (18), and recently multiple peptides in human plasma samples have been measured simultaneously by application of the MRM strategy

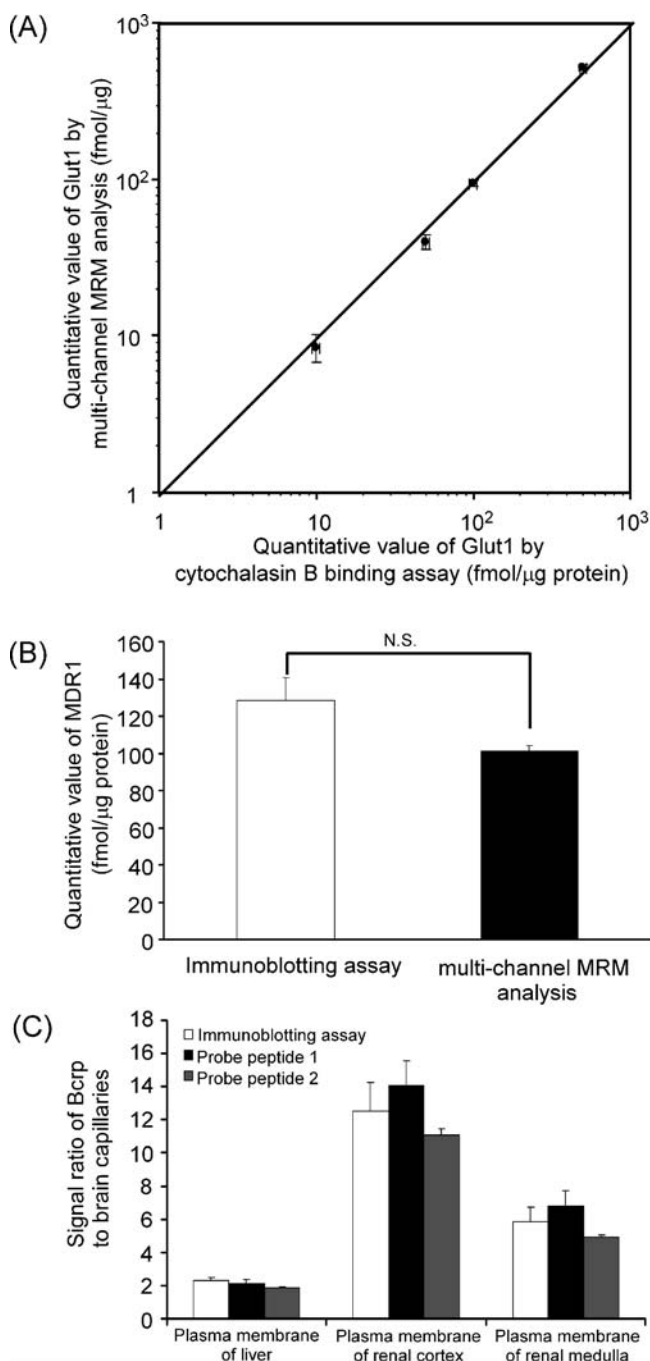


**Fig. 6.** Comparison of quantitative values between multi-channel MRM analysis and binding or immunoblotting assay. **A** Protein amounts of Glut1 in mouse brain capillary endothelial cells were quantified by multi-channel MRM analysis and cytochalasin B binding assay. Each point represents the mean  $\pm$  SEM ( $n=4$ ). **B** Protein amounts of human MDR1 in pig kidney cells expressing human MDR1 were quantified by quantitative western blotting and multi-channel MRM analysis. Each value represents the mean  $\pm$  SD ( $n=4-6$ ). **C** Relative amounts of Bcrp in mouse tissues to that of brain capillary endothelial cells determined by immunoblotting and by multi-channel MRM analysis with two different probe peptides. The amino acid sequences of probe peptides 1 and 2 were SLLLDVLAAR and ENLQFSAALR, respectively. Each value represents the mean  $\pm$  SEM ( $n=6$ ). *N.S.* No significant difference ( $p>0.05$ ).

(16,20). However, no one has previously succeeded in developing a simultaneous and direct quantitation method for multiple membrane proteins in mammalian tissues using MRM analysis.

The present study has solved critical issues for applying MRM analysis to such proteins by the use of *in-silico* selection of probe peptides. Proteins give rise to tens or hundreds of tryptic peptides, and only some of these peptides are suitable for quantitative analysis. For example, as shown in Fig. 2, the ion intensities of the peptides derived from HSA vary widely, and only peptides giving sufficiently high ion intensities provide low CVs. The requirements for a usable peptide are as follows: (1) can be detected by LC-ESI-MS/MS analysis with sufficient sensitivity, (2) efficiently generated by enzymatic digestion, (3) specific to the target protein. The target proteins were digested with trypsin *in-silico*, and target peptides were chosen on the basis of the selection criteria in Table I. The first selection deals with the requirements for measurement with a mass spectrometer. The probe peptides should be 6–16 amino acids in length, because the  $m/z$  values of their doubly charged precursor ions are below 1,000, lying within the detectable mass range (5 to 1,250  $m/z$ ) of the mass spectrometer (API5000). The probe sequence should have no posttranslational modification or polymorphism, to minimize mass variations. However, when a modified or mutated protein is to be quantified, the probe peptide should contain the modification or mutation site, and multi-channel MRM analysis can be used to distinguish the single amino acid difference and/or modification. Peptides containing methionine or cysteine were excluded to avoid the possibility of chemical modifications during operation. Sequences containing transmembrane domains and stretches of arginine or lysine residues were also excluded, since the efficiency of trypsin digestion can be very low in such regions (32). Moreover, tandem sequences of hydrophobic amino acids in transmembrane domains are likely to result in low ion intensity. Peptides containing leucine, isoleucine, valine, alanine and proline are suitable for stable isotope-labeling. Then, the probe peptide was selected from among the candidate peptides by the second selection, focusing on the need for sensitive detection by LC-ESI-MS/MS. In the second selection, peptides with a histidine residue were excluded, because the sensitivity of ESI-MS analysis to such peptides is low (33). Also, an amino acid residue number 8 to 10 was given priority, because then doubly charged precursor ions appear at less than 700  $m/z$ , which is in the more sensitive range of the API5000. All of the peptides selected showed strong ion intensities and low CVs at 10 fmol, whereas the ion intensities of all peptides derived from HSA were much more variable (Fig. 2). This result demonstrates that our *in-silico* approach is a useful method for selecting peptides for highly sensitive quantitative analysis.

Analyte peaks are usually identified by the chromatographic retention time of an internal reference in single MRM recordings. However, in some cases there are secondary peaks in MRM recordings, and it is difficult to identify small signal peaks (20). The present method overcomes this problem by employing multi-channel MRM analysis with three MRM channels derived from different product ions of the probe peptide (Fig. 4). Figure 5 shows that specific signal peaks for SLLLDVLAAR peptide derived from Bcrp could

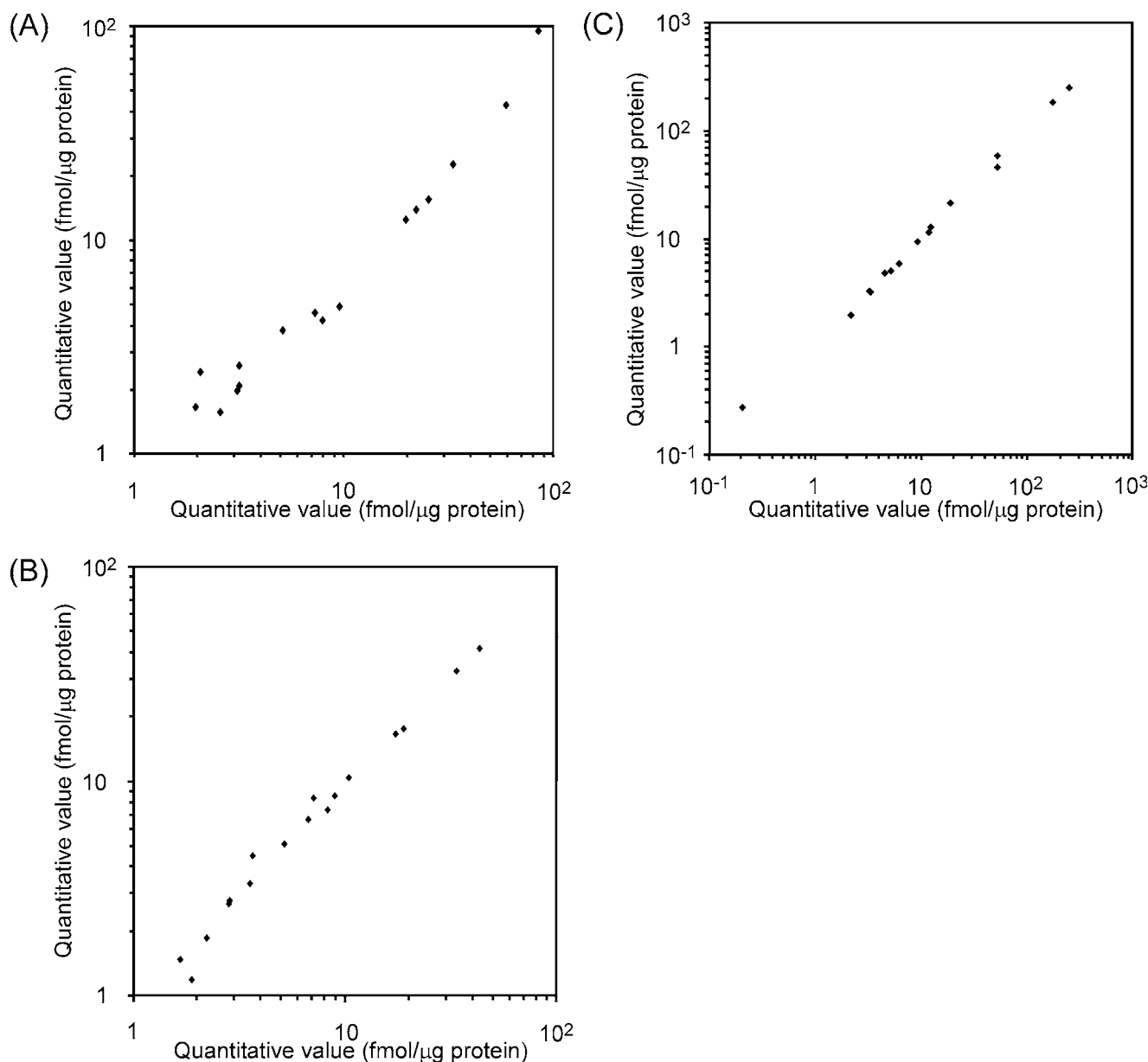


**Fig. 7.** Reproducibility of quantitative values obtained by multi-channel MRM analysis. Two aliquots of one sample from mouse brain capillary endothelial cells (**A**), plasma membrane of liver (**B**) or renal cortex (**C**) were separately digested with trypsin (digest A and digest B). Isotope-labeled peptide (200 fmol) was added to the digest, followed by multi-channel MRM analysis. The quantitative values for 38 peptides in the two replicate digests were plotted against each other. Each *point* represents the mean value ( $n=6$ ).

be identified in the liver sample because of the correspondence of the retention times in all channels, despite the fact that many peaks were detected in the analyte and internal reference channels. If each gap between Q3 masses in the y or b series ions of a peptide corresponds to one amino acid, the three MRM channels define a two amino acid sequence. The probability of a given two amino acid sequence for twenty amino acids is one in four hundred. Therefore, multiple channels are useful for correct identification of signal peaks derived from low-expression proteins in biological samples with high matrix backgrounds. The multi-channel MRM analysis is also important to obtain reliable quantitative

values. In the analysis of the mouse tissues, all quantitative values determined from three peaks of peak area over 5,000 counts gave CVs of less than 20.0% (Table V), whereas only 30.8% of the quantitative values determined from two peaks of peak area over 5,000 counts showed CVs of less than 20.0% (data not shown).

Sample preparation for LC-MS/MS includes denaturing, protein precipitation and trypsin digestion processes. To assess the effect of the preparation procedures, the quantitative values were compared between peptide-based quantification by multi-channel MRM analysis and protein-based quantification by binding assay or immunoblotting assay. MDR1 and

Glut1 are glycosylated membrane proteins containing 12 transmembrane domains and consisting of 1,280 and 492 amino acid, respectively. Bcrp is a glycosylated membrane protein with six transmembrane domains, consisting of 657 amino acid, and forms a homo-dimer. For these large membrane proteins, no significant difference was observed between the two methods (Fig. 6). Furthermore, no bands over 20 kDa were detected by SDS-PAGE after trypsin digestion (data not shown), and two different probe peptides for either Mdr1a or Bcrp gave quantitative values that were not significantly different (Table V), suggesting efficient digestion by trypsin. Thus, we consider that the sample preparation procedures do not significantly affect the quantitative values determined by multi-channel MRM analysis, although we cannot exclude the possibility that the efficiency of the preparation procedures is inadequate for some proteins.

To quantify protein expression levels of transporters in plasma membrane fraction, as shown in liver and kidney in Table V, the purity/quality of the fraction is an important issue, since it will influence the estimated levels of transporters. Two approaches to this problem can be considered; one is to quantify transporters in whole cell lysate, instead of plasma membrane fraction, and then to normalize transporter expression levels by total protein amount. The other is to quantify simultaneously transporters and plasma membrane markers, such as Na<sup>+</sup>/K<sup>+</sup> ATPase (Atp4a) and  $\gamma$ -glutamyl transpeptidase (Ggt1), and then to normalize transporter expression levels with respect to these markers. Since it seems preferable to measure the expression levels in plasma membrane by using plasma membrane fraction, rather than whole cells, the latter approach could be the better one to evaluate transporter expression in a single tissue or to compare levels in different tissues, provided that they exhibit similar expression levels of the marker protein(s). Since the expression levels of the marker Atp4a were greater in the kidney than in other tissues (Table V), further studies are needed to identify a better plasma membrane marker(s), and multi-channel MRM analysis is expected to be a good technique for finding such marker(s).

This is the first report to describe the quantitative absolute protein expression profiles of multiple transporters in mouse tissues. Using the multi-channel MRM analysis, we were able to quantify Mdr1a, Mrp4, Bcrp, 4F2hc, Asct2, Glut1, Mct1, Lat1, Oat3, Oatp2, Oatpf, Taut in brain capillary endothelial cells, Bsep, Mrp2, Mrp3, Mrp6, Bcrp, Abcg5, Abcg8, 4F2hc, Nat, Gat2, Glut1, Mct1, Ntcp, Oatp1 and Oatp2 in liver, and Mrp2, Mrp4, Bcrp, 4F2hc, Asct2, Mct1, Oat1, Oat3, Oatp1, Taut and Mate1 in kidney, with low CV values (Table V). These transporters have been reported to be functionally expressed in these tissues (5,6,8,34). This result demonstrates that multi-channel MRM analysis has sufficient sensitivity to determine the protein amounts of functionally important transporters in mammalian tissues.

Mdr1a was below the detection limit in the liver and kidney (<0.43 and <0.25 fmol/ $\mu$ g protein, respectively) and its expression level in brain capillaries was at least 30- and 51-fold greater than in the liver and kidney, respectively. A previous western blot analysis by Conrad *et al.* (35) showed

that P-glycoprotein was detected more abundantly in the membrane fraction (though not the capillaries) of the brain than in the corresponding fractions of liver and kidney. This western blot result is not inconsistent with the present findings. We also confirmed that the relative protein expression levels of Bcrp detected by western blotting were consistent with the results obtained by multi-channel MRM analysis among brain capillaries, liver and kidney (Fig. 6). In mdr1a/b knockout mice, Schinkel *et al.* (36) reported that accumulation of digoxin in brain was 27-fold greater in mdr1a/b knockout mice than in wild-type mice, while it was 2.6- and 2.5-fold greater in the kidney and liver, respectively. These functional data are broadly consistent with the protein expression levels in each tissue found in the present study. Furthermore, multi-channel MRM analysis can distinguish mdr1a and mdr1b at the protein level, whereas the two are difficult to distinguish with antibodies, even though western blotting may have higher sensitivity.

In this analysis, 36 proteins were quantified simultaneously. It is possible to construct 300 MRM channels in a single analysis with the API5000 mass spectrometer that we used. Therefore, a maximum of 50 proteins can be quantified simultaneously with three-channel-per-protein MRM analysis using this instrument. This highly sensitive, simultaneous quantification method combined with our novel *in-silico* peptide selection criteria for membrane proteins should make it possible to construct a quantitative atlas of membrane proteins, including transporters, receptors and enzymes, in humans and other species. A key bottleneck in drug discovery and development is the time taken to move from preclinical to clinical studies, and quantitative proteomics-based pharmacokinetics, i.e., pharmacoproteomics, may lead to rational strategies to minimize this delay.

Many transporters, channels and receptors have been identified in the plasma membranes of tissues, and are thought to play important roles in disease processes and drug absorption/distribution/elimination in animals and humans. Because of their importance in drug development, the expression profiles of transporters have been analyzed at the mRNA level in pharmacogenomic studies (8,37–40). However, mRNA expression levels do not necessarily correlate with protein amounts at the plasma membrane. Since the established *in-silico* selection and multi-channel MRM analysis is applicable to receptors, channels and cytosolic proteins, the method described here provides a means to move from pharmacogenomics to pharmacoproteomics, and this should in turn lead to improved strategies of drug discovery and development.

In conclusion, we have developed a highly sensitive and simultaneous quantification method for membrane proteins, e.g., transporter, enzyme, by LC tandem mass spectrometry with multi-channel MRM analysis. We also developed an *in-silico* design method for an appropriate peptide in the LC/MS/MS quantification. The method was validated, and applied to construct a quantitative atlas of membrane transporter and enzyme proteins in brain capillary endothelial cells, liver and kidney of the mouse. This approach makes it possible to compare protein expression profiles of membrane proteins or other proteins expressed at low levels in various tissues, and should have many potential applications.

## ACKNOWLEDGEMENTS

We would like to thank Ms N. Funayama for secretarial assistance. This study was supported in part by a Grant-in-Aid for Young Scientist (B) and Scientific Research on Priority Areas (17081002) from the Ministry of Education, Culture, Sports, Science and Technology of Japan, and Grant-in-Aid for Scientific Research (S), Scientific Research (B) and a 21st Century Center of Excellence (COE) Program grant from the Japan Society for the Promotion of Science. This study was also supported in part by the Industrial Technology Research Grant Program from New Energy and the Industrial Technology Development Organization (NEDO) of Japan.

## REFERENCES

- J. Nezu, I. Tamai, A. Oku, R. Ohashi, H. Yabuuchi, N. Hashimoto, H. Nikaïdo, Y. Sai, A. Koizumi, Y. Shoji, G. Takada, T. Matsuishi, M. Yoshino, H. Kato, T. Ohura, G. Tsujimoto, J. Hayakawa, M. Shimane, and A. Tsuji. Primary systemic carnitine deficiency is caused by mutations in a gene encoding sodium ion-dependent carnitine transporter. *Nat. Genet.* **21**:91–94 (1999).
- M. J. Welsh, and A. E. Smith. Molecular mechanisms of CFTR chloride channel dysfunction in cystic fibrosis. *Cell* **73**:1251–1254 (1993).
- J. Kartenbeck, U. Leuschner, R. Mayer, and D. Keppler. Absence of the canalicular isoform of the MRP gene-encoded conjugate export pump from the hepatocytes in Dubin–Johnson syndrome. *Hepatology* **23**:1061–1066 (1996).
- G. Szakacs, J. K. Paterson, J. A. Ludwig, C. Booth-Genthe, and M. M. Gottesman. Targeting multidrug resistance in cancer. *Nat. Rev. Drug Discov.* **5**:219–234 (2006).
- N. Mizuno, T. Niwa, Y. Yotsumoto, and Y. Sugiyama. Impact of drug transporter studies on drug discovery and development. *Pharmacol. Rev.* **55**:425–461 (2003).
- A. Tsuji. Impact of transporter-mediated drug absorption, distribution, elimination and drug interactions in antimicrobial chemotherapy. *J. Infect. Chemother.* **12**:241–250 (2006).
- Y. Shitara, T. Horie, and Y. Sugiyama. Transporters as a determinant of drug clearance and tissue distribution. *Eur. J. Pharm. Sci.* **27**:425–446 (2006).
- S. Ohtsuki, and T. Terasaki. Contribution of carrier-mediated transport systems to the blood–brain barrier as a supporting and protecting interface for the brain; Importance for CNS drug discovery and development. *Pharm. Res.* **24**:1745–1758 (2007).
- R. Aebersold, and M. Mann. Mass spectrometry-based proteomics. *Nature* **422**:198–207 (2003).
- S. D. Patterson, and R. H. Aebersold. Proteomics: the first decade and beyond. *Nat. Genet.* **33**(Suppl):311–323 (2003).
- B. Domon, and R. Aebersold. Mass spectrometry and protein analysis. *Science* **312**:212–217 (2006).
- H. Steen, and A. Pandey. Proteomics goes quantitative: measuring protein abundance. *Trends Biotechnol.* **20**:361–364 (2002).
- S. E. Ong, L. J. Foster, and M. Mann. Mass spectrometric-based approaches in quantitative proteomics. *Methods* **29**:124–130 (2003).
- S. P. Gygi, B. Rist, S. A. Gerber, F. Turecek, M. H. Gelb, and R. Aebersold. Quantitative analysis of complex protein mixtures using isotope-coded affinity tags. *Nat. Biotechnol.* **17**:994–999 (1999).
- J. A. Ranish, E. C. Yi, D. M. Leslie, S. O. Purvine, D. R. Goodlett, J. Eng, and R. Aebersold. The study of macromolecular complexes by quantitative proteomics. *Nat. Genet.* **33**:349–355 (2003).
- L. Anderson, and C. L. Hunter. Quantitative mass spectrometric multiple reaction monitoring assays for major plasma proteins. *Mol. Cell. Proteomics* **5**:573–588 (2006).
- G. Marko-Varga, H. Lindberg, C. G. Lofdahl, P. Jonsson, L. Hansson, M. Dahlback, E. Lindquist, L. Johansson, M. Foster, and T. E. Fehniger. Discovery of biomarker candidates within disease by protein profiling: principles and concepts. *J. Proteome Res.* **4**:1200–1212 (2005).
- D. R. Barnidge, E. A. Dratz, T. Martin, L. E. Bonilla, L. B. Moran, and A. Lindall. Absolute quantification of the G protein-coupled receptor rhodopsin by LC/MS/MS using proteolysis product peptides and synthetic peptide standards. *Anal. Chem.* **75**:445–451 (2003).
- S. A. Gerber, J. Rush, O. Stemman, M. W. Kirschner, and S. P. Gygi. Absolute quantification of proteins and phosphoproteins from cell lysates by tandem MS. *Proc. Natl. Acad. Sci. USA* **100**:6940–6945 (2003).
- H. Keshishian, T. Addona, M. Burgess, E. Kuhn, and S. A. Carr. Quantitative, multiplexed assays for low abundance proteins in plasma by targeted mass spectrometry and stable isotope dilution. *Mol. Cell. Proteomics* **6**:2212–2229 (2007).
- J. S. Andersen, C. J. Wilkinson, T. Mayor, P. Mortensen, E. A. Nigg, and M. Mann. Proteomic characterization of the human centrosome by protein correlation profiling. *Nature* **426**:570–574 (2003).
- S. Hori, S. Ohtsuki, M. Tachikawa, N. Kimura, T. Kondo, M. Watanabe, E. Nakashima, and T. Terasaki. Functional expression of rat ABCG2 on the luminal side of brain capillaries and its enhancement by astrocyte-derived soluble factor(s). *J. Neurochem.* **90**:526–536 (2004).
- R. J. Boado, and M. M. Pardridge. A one-step procedure for isolation of poly(A) mRNA from isolated brain capillaries and endothelial cells in culture. *J. Neurochem.* **57**:2136–2139 (1991).
- W. M. Pardridge, R. J. Boado, and C. R. Farrell. Brain-type glucose transporter (GLUT-1) is selectively localized to the blood–brain barrier. Studies with quantitative western blotting and *in situ* hybridization. *J. Biol. Chem.* **265**:18035–18040 (1990).
- K. G. Mawuenyega, H. Kaji, Y. Yamuchi, T. Shinkawa, H. Saito, M. Taoka, N. Takahashi, and T. Isobe. Large-scale identification of *Caenorhabditis elegans* proteins by multidimensional liquid chromatography–tandem mass spectrometry. *J. Proteome Res.* **2**:23–35 (2003).
- P. Chen, X. Li, Y. Sun, Z. Liu, R. Cao, Q. He, M. Wang, J. Xiong, J. Xie, X. Wang, and S. Liang. Proteomic analysis of rat hippocampal plasma membrane: characterization of potential neuronal-specific plasma membrane proteins. *J. Neurochem.* **98**:1126–1140 (2006).
- K. Nagano, M. Taoka, Y. Yamauchi, C. Itagaki, T. Shinkawa, K. Nunomura, N. Okamura, N. Takahashi, T. Izumi, and T. Isobe. Large-scale identification of proteins expressed in mouse embryonic stem cells. *Proteomics* **5**:1346–1361 (2005).
- A. V. Pshezhetsky, M. Fedjaev, L. Ashmarina, A. Mazur, L. Budman, D. Sinnott, D. Labuda, J. F. Beaulieu, D. Menard, I. Nifant'ev, and E. Levy. Subcellular proteomics of cell differentiation: quantitative analysis of the plasma membrane proteome of Caco-2 cells. *Proteomics* **7**:2201–2215 (2007).
- E. Kuhn, J. Wu, J. Karl, H. Liao, W. Zolg, and B. Guild. Quantification of C-reactive protein in the serum of patients with rheumatoid arthritis using multiple reaction monitoring mass spectrometry and 13C-labeled peptide standards. *Proteomics* **4**:1175–1186 (2004).
- S. L. Wu, H. Amato, R. Biringer, G. Choudhary, P. Shieh, and W. S. Hancock. Targeted proteomics of low-level proteins in human plasma by LC/MSn: using human growth hormone as a model system. *J. Proteome Res.* **1**:459–465 (2002).
- D. R. Barnidge, M. K. Goodmanson, G. G. Klee, and D. C. Muddiman. Absolute quantification of the model biomarker prostate-specific antigen in serum by LC-MS/MS using protein cleavage and isotope dilution mass spectrometry. *J. Proteome Res.* **3**:644–652 (2004).
- D. D. Sabatini, and G. Blobel. Controlled proteolysis of nascent polypeptides in rat liver cell fractions. II. Location of the polypeptides in rough microsomes. *J. Cell. Biol.* **45**:146–157 (1970).
- P. Mallick, M. Schirle, S. S. Chen, M. R. Flory, H. Lee, D. Martin, J. Ranish, B. Raught, R. Schmitt, T. Werner, B. Kuster, and R. Aebersold. Computational prediction of proteotypic peptides for quantitative proteomics. *Nat. Biotechnol.* **25**:125–131 (2007).
- S. Ohtsuki. New aspects of the blood–brain barrier transporters; its physiological roles in the central nervous system. *Biol. Pharm. Bull.* **27**:1489–1496 (2004).

35. S. Conrad, A. Viertelhaus, A. Orzechowski, J. Hoogstraate, K. Gjellan, D. Schrenk, and H. Kauffmann. Sequencing and tissue distribution of the canine MRP2 gene compared with MRP1 and MDR1. *Toxicology* **156**:81–91 (2001).
36. A. H. Schinkel, U. Mayer, E. Wagenaar, C. A. A. Mol, L. Deemter, J. M. Zijlmans, W. E. Fibbe, and P. Borst. Normal viability and altered pharmacokinetics in mice lacking mdr1-type (drug-transporting) P-glycoproteins. *Proc. Natl. Acad. Sci. USA* **94**:4028–4033 (1997).
37. Y. Huang. Pharmacogenetics/genomics of membrane transporters in cancer chemotherapy. *Cancer Metastasis Rev.* **26**:183–201 (2007).
38. J. König, A. Seithel, U. Gradhand, and M. F. Fromm. Pharmacogenomics of human OATP transporters. *Naunyn Schmiedebergs Arch. Pharmacol.* **372**:432–443 (2006).
39. C. Hilgendorf, G. Ahlin, A. Seithel, P. Artursson, A. L. Ungell, and J. E. Karlsson. Expression of thirty-six drug transporter genes in human intestine, liver, kidney, and organotypic cell lines. *Drug Metab. Dispos.* **35**:1333–1340 (2007).
40. T. Terasaki, and S. Ohtsuki. Brain-to-blood transporters for endogenous substrates and xenobiotics at the blood–brain barrier: an overview of biology and methodology. *NeuroRx* **2**:63–72 (2005).